



Best practices and methods

Ammonia-based green corridors for sustainable maritime transportation

Hanchu Wang, Prodromos Daoutidis*, Qi Zhang*

Department of Chemical Engineering and Materials Science, University of Minnesota, Minneapolis, MN 55455, USA



ARTICLE INFO

Keywords:

Green ammonia
Alternative marine fuel
Maritime transportation
Green corridors
Supply chain design

ABSTRACT

Decarbonizing maritime transportation will require huge investments in new technologies and infrastructure for the production, distribution, and utilization of alternative marine fuels. In this context, the concept of green shipping corridors has been proposed, where a green corridor refers to a major shipping route along which low- and zero-carbon maritime transportation solutions are provided. In this work, we conduct a global analysis of green shipping corridors by designing a network of alternative fuel production sites, transportation links, and bunkering ports that can support a large fraction of the global marine fuel demand. We choose green ammonia to be the alternative fuel as it has received significant attention as a potential carbon- and sulfur-free marine fuel that can be produced entirely from renewable resources. Our study identifies the most suitable locations for producing and bunkering green ammonia, examines the trade-off between ammonia production and transportation costs, and highlights the extent to which local reduction in production cost can lead to a competitive advantage in a future green ammonia market. We also demonstrate the value of our global network optimization, which considers many shipping routes simultaneously, in capturing potential synergies and trade-offs across different routes and regions. This work provides insights that can help inform decisions in establishing future green shipping corridors around the world.

1. Introduction

Maritime transportation is essential to the global economy as it enables the distribution of more than 80% in volume and 70% in value of internationally traded products (UNCTAD, 2018). However, it is also currently responsible for about 3% of global annual greenhouse gas (GHG) emissions. Following the Paris Agreement, the International Maritime Organization (IMO) has announced the goal of reducing the international shipping sector's annual GHG emissions by at least 50% compared to 2008 by 2050 (IMO, 2018). This urgent need to decarbonize the shipping industry has inspired the concept of *green shipping corridors* (Getting to Zero Coalition, 2021), which refer to major shipping routes that are supported by or provide favorable conditions for low- and zero-carbon maritime transportation solutions. The goal of creating such green corridors is to promote and accelerate the implementation of sustainable marine fuels and technologies. This idea has gained much attention recently, and governments are working toward the development of green corridors as the first step toward achieving zero GHG emissions in all aspects of maritime shipping (U.S. Department of State, 2022).

The primary source of emissions from marine operations is the combustion of marine fuel; thus, replacing the current fossil fuels with cleaner alternatives is the primary objective. A green corridor encompasses the infrastructure and operational capabilities that enable the

production, distribution, and utilization of alternative marine fuels. The main components are fuel production facilities, ports with fuel storage capacities, transportation links between production facilities and ports, and bunkering infrastructure. These are all major investments that potentially need to take place in multiple countries; hence, effective coordination will be key in establishing green shipping corridors.

In terms of clean alternative marine fuels, ammonia has been identified as one of the most promising candidates (Hansson et al., 2020). Ammonia can serve as a hydrogen carrier or directly be used as a fuel in internal combustion engines (Cardoso et al., 2021) or fuel cells (Adli et al., 2018; Wojcik et al., 2003). It has a relatively high energy density, and since it is an inorganic molecule that only contains hydrogen and nitrogen, there is no emission of CO₂ or sulfur oxides when it is combusted. Importantly, ammonia can be produced in a green fashion, for example, using hydrogen from water electrolysis and nitrogen from air separation, with the entire process powered by renewable electricity (Baltrusaitis, 2017; Wang et al., 2018; MacFarlane et al., 2020). In the U.S., one of the world's first wind-to-ammonia pilot plants began operation in 2013 (Reese et al., 2016). Worldwide, since 2018, more than 60 renewable ammonia plants with a combined annual capacity of 15 Mt have been announced, which is only expected to further increase in the coming years (IRENA and AEA, 2022). Another

* Corresponding authors.

E-mail addresses: daout001@umn.edu (P. Daoutidis), qizh@umn.edu (Q. Zhang).

advantage of ammonia is that, since it is one of the world's most widely produced chemicals, there is already a well-established global ammonia storage and distribution infrastructure, as well as training, industry codes, and safety regulations. Challenges in the use of ammonia as a fuel, including its low flame velocity when combusted and the associated nitrogen oxide emissions, still exist; however, there have been significant efforts in developing remedies to overcome these issues in recent years (Erdemir and Dincer, 2021; Jeerh et al., 2021). Earlier in 2022, the world's first ammonia-ready tanker was delivered, marking an important milestone in the maritime industry's evolution toward utilizing alternative marine fuels (Prevljak, 2022).

In a recent report by the [Getting to Zero Coalition \(2021\)](#), multiple shipping routes have been identified as potentially suitable green corridors. While the report provides a quantitative but rather high-level analysis, it offers important insights into the requirements for green corridors and motivates further, more detailed studies. In our work, we aim to provide a global, more integrated picture of potential green corridors. To this end, we conduct a comprehensive supply chain analysis in which we design a global network of ammonia-based green corridors. Using a spatially explicit supply chain model, we optimize the locations of the green ammonia production plants and refueling ports, the required fuel transportation, storage, and bunkering infrastructure, as well as the shipping routes themselves. By considering a network of green corridors rather than analyzing fixed individual green corridors separately, our model is able to capture potential synergies across different routes and geographical regions. To the best of our knowledge, this is the first analysis of green shipping corridors of this kind, especially at this level of detail and scale.

The remainder of this paper is organized as follows. In Section 2, a literature review of related works is presented. We describe our methodology, including the formulation of our supply chain model and details about the data used in our study, in Section 3. A detailed discussion of the results is presented in Section 4 before we close with some concluding remarks in Section 5.

2. Literature review

While systems-level analyses of green ammonia used as marine fuel are scarce, there is a rapidly growing body of systems engineering work on green ammonia in general ([Palys et al., 2021](#)). Here, most existing works study the techno-economics of producing green ammonia ([Sánchez and Martín, 2018](#); [Palys et al., 2018](#); [Demirhan et al., 2019](#); [Wang et al., 2020](#); [Zhang et al., 2020](#); [Nayak-Luke and Bañares-Alcántara, 2020](#); [Tang et al., 2022](#)), yet there is an increasing focus on investigating different ways of utilizing green ammonia, not only as fertilizer ([Wang et al., 2021b](#)) but also as a hydrogen and energy carrier. In its role as an energy vector ([Salmon and Bañares-Alcántara, 2021](#)), ammonia can be used in various applications, e.g. for power generation ([Cesaro et al., 2021](#); [Sánchez et al., 2021a](#)), heating ([Palys et al., 2021](#)), as tractor fuel ([Palys et al., 2019b](#)), and generally for energy storage ([Wang et al., 2017](#); [Palys and Daoutidis, 2020](#); [Wang et al., 2021a](#)). [Al-Aboosi et al. \(2021\)](#) discussed the technical and economic feasibility of green ammonia as a marine fuel but provided a rather high-level analysis. For the design of green ammonia systems that involve the use of intermittent renewable energy resources such as solar and wind, it is important to consider detailed plant operations in order to determine adequate plant capacities. This aspect was investigated early on ([Beerbühl et al., 2015](#); [Allman et al., 2019](#)) and has now become the norm in the techno-economic analysis of green ammonia systems. Similarly, one needs to consider seasonal changes in renewable resource availability and ammonia demand as well as inventory management over the course of a year; this, for example, is crucial when considering the highly seasonal application of ammonia as fertilizer ([Wang et al., 2021b](#)) or studying the potential benefits of ammonia for long-term energy storage ([Palys and Daoutidis, 2020](#)).

Green ammonia has also been studied at the supply chain level. [Allman et al. \(2017\)](#) proposed a framework for ammonia supply chain optimization incorporating conventional and renewable generation and considering both economic and environmental objectives. They demonstrated the importance of plant scale and studied the impact of a carbon tax on the design of the ammonia supply chain. Motivated by the distributed availability of renewable energy, [Palys et al. \(2019a\)](#) explored the potential benefits of modular, wind-powered ammonia production by considering it in a distributed supply chain and accounting for per-module cost reduction as the number of built modules increases. While earlier works mostly analyzed ammonia supply chains for the purpose of satisfying agricultural demand, more recent studies focused on ammonia's role as a hydrogen and energy carrier that is relatively easy to store and to transport. For instance, [Obara \(2019\)](#) investigated the potential of ammonia as a hydrogen carrier by analyzing the energy and exergy flows in a hydrogen-energy supply chain. [Ogumerem et al. \(2019\)](#) designed an ammonia supply network for the State of Texas to investigate the future economic viability of chemically storing renewable energy to displace electricity generated from fossil fuels. A similar approach was taken by [Sánchez et al. \(2021b\)](#), who considered ammonia, together with other chemical storage media, for a specific region in Spain; their proposed supply chain optimization framework also accounts for detailed plant operations. Further increasing the spatial scope, [Salmon et al. \(2021\)](#) considered ammonia as a means to transport energy between different continents; one interesting finding from this study is that despite the low transportation cost relative to the production cost of ammonia, the optimal distribution of green ammonia tends to occur on regional scales rather than over ultralong distances.

From an optimization modeling standpoint, our work is most closely related to the literature on the design of refueling station networks, most commonly considered in the context of alternative fuel vehicles, including electric cars and fuel cell vehicles. Most refueling station location models assume that the fuel is readily available and only consider the placement of refueling stations given vehicle demands. Based on how demands are represented, existing model formulations can be broadly categorized as models with node-based demands and models with path-based demands ([Honma and Kuby, 2019](#)). Problems with node-based demands are commonly modeled using classical facility location formulations ([Bapna et al., 2002](#); [Wang, 2007](#)). In the path-based approach, each demand is associated with a trip defined by its origin and destination, and a demand is assumed to be covered by a refueling station if the refueling station is located on its path. Path-based demand representation is often considered more suitable in capturing realistic refueling behavior ([Honma and Kuby, 2019](#)) and has led to the development of the so-called flow-capturing location model ([Berman et al., 1992](#); [Hodgson, 1990](#)) and a number of extensions thereof ([Kuby and Lim, 2005](#); [Kim and Kuby, 2012](#); [Shukla et al., 2011](#); [Arslan et al., 2019](#)).

The above-mentioned refueling station location models have mostly been used in applications involving ground vehicles. More recently, they have also been extended to address similar problems in maritime transportation, primarily for the design of networks of liquified natural gas (LNG) bunkering ports. The majority of LNG supply chain problems are formulated as facility location problems, where they mention the potential use of LNG as marine fuel but do not explicitly model shipping routes and marine fuel demands ([Jokinen et al., 2015](#); [Bittante et al., 2018](#); [Alvarez et al., 2020](#)). An exception is the work by [Ursavas et al. \(2020\)](#), who used a modified flow-capturing location model to optimize the design of an LNG bunkering network, considering both truck-to-ship and pipeline-to-ship bunkering. Ship-to-ship bunkering was considered by [Doymus et al. \(2022\)](#), who applied a multiperiod planning formulation to simultaneously optimize the fleet of bunker barges and the routing of those barges.

3. Methodology

The large majority of existing works on refueling station location only focus on fuel distribution and do not consider fuel production. In the case of green ammonia as an alternative marine fuel, however, the production cost can vary significantly across different locations such that the choice of production sites may also affect the location of the bunkering ports. Hence, in this work, we consider the design of global ammonia-based green corridors that include both the network of bunkering ports and the ammonia production plants that supply the fuel. In the following, we present our optimization model, which combines a facility location formulation (Tragantalerngsak et al., 2000) with a flow-capturing location formulation (Kuby and Lim, 2005), and a detailed description of the data and assumptions used in the model. Note that all continuous variables in the proposed model are specified to be nonnegative. A nomenclature with all sets, parameters, and variables can be found in the supplementary material.

3.1. Model formulation

We consider a set of candidate bunkering ports \mathcal{J} and a set of path-based shipping demands \mathcal{Q} , where each shipping demand $q \in \mathcal{Q}$ is defined by its fuel demand γ_q and the set of potential bunkering ports on its shipping route $\bar{\mathcal{J}}_q \subseteq \mathcal{J}$. We further consider a set of candidate green ammonia production sites \mathcal{I} , and at each site $i \in \mathcal{I}$, we allow the construction of potentially multiple green ammonia plants; this set of candidate plants at site i is denoted by \mathcal{H}_i . For all plants, we assume the same green ammonia manufacturing process, which uses water electrolysis to produce hydrogen and air separation to produce nitrogen, which are then reacted to form ammonia in a Haber–Bosch synthesis process. Additionally, for offshore sites, seawater purification and offshore platform construction are considered. There are potentially multiple sources of renewable electricity, e.g. solar and wind, from which one can choose; we denote this set of renewable energy sources available at production site i by \mathcal{M}_i .

The production capacity constraints at the potential plant locations are formulated as follows:

$$\sum_{j \in \mathcal{J}} w_{ij} \leq \sum_{h \in \mathcal{H}_i} C_{ih} \quad \forall i \in \mathcal{I} \quad (1)$$

$$C_{ih}^{\min} p_{ih} \leq C_{ih} \leq C_{ih}^{\max} p_{ih} \quad \forall i \in \mathcal{I}, h \in \mathcal{H}_i \quad (2)$$

$$p_{ih} \leq p_{i,h-1} \quad \forall i \in \mathcal{I}, h \in \mathcal{H}_i \setminus \{1\} \quad (3)$$

$$p_{ih} \in \{0, 1\} \quad \forall i \in \mathcal{I}, h \in \mathcal{H}_i, \quad (4)$$

where w_{ij} denotes the amount of ammonia transported from site i to port j , C_{ih} is the production capacity of plant $h \in \mathcal{H}_i$, C_{ih}^{\min} and C_{ih}^{\max} are the minimum and maximum capacities of plant $h \in \mathcal{H}_i$, respectively, and the binary variable p_{ih} equals 1 if plant h is built at site i . Constraints (1) state that the produced amount of ammonia at each site cannot exceed the installed production capacity at that site. The size of each plant is restricted by inequalities (2). Furthermore, symmetry-breaking constraints are added in the form of constraints (3).

The production of green ammonia at each site is enabled by electricity generated from renewable resources. The following constraints ensure that sufficient renewable power generation capacity is installed:

$$E_{im}^{\min} z_{im} \leq E_{im} \leq E_{im}^{\max} z_{im} \quad \forall i \in \mathcal{I}, m \in \mathcal{M}_i \quad (5)$$

$$\sum_{m \in \mathcal{M}_i} E_{im} \geq \rho_i \sum_{h \in \mathcal{H}_i} C_{ih} \quad \forall i \in \mathcal{I} \quad (6)$$

$$z_{im} \in \{0, 1\} \quad \forall i \in \mathcal{I}, m \in \mathcal{M}_i, \quad (7)$$

where E_{im} denotes the electricity generation capacity from source m at site i , E_{im}^{\min} and E_{im}^{\max} are the minimum and maximum generation capacities, respectively, the binary variable z_{im} equals 1 if renewable source m is chosen at site i , and ρ_i is the amount of electricity consumed for producing one unit of ammonia at site i .

Ammonia is transported from the production plants to the bunkering ports. The binary variable x_{ij} equals 1 if ammonia is transported from plant i to port j , which is enforced by the following constraints:

$$w_{ij} \leq \sum_{h \in \mathcal{H}_i} C_{ih}^{\max} x_{ij} \quad \forall i \in \mathcal{I}, j \in \mathcal{J} \quad (8)$$

$$x_{ij} \in \{0, 1\} \quad \forall i \in \mathcal{I}, j \in \mathcal{J}. \quad (9)$$

The bunkering capacity and ammonia balance constraints at the potential bunkering port locations are formulated as follows:

$$\sum_{i \in \mathcal{I}} w_{ij} \leq \bar{C}_j \quad \forall j \in \mathcal{J} \quad (10)$$

$$\bar{C}_j^{\min} b_j \leq \bar{C}_j \leq \bar{C}_j^{\max} b_j \quad \forall j \in \mathcal{J} \quad (11)$$

$$\sum_{i \in \mathcal{I}} w_{ij} = \sum_{q \in \bar{\mathcal{Q}}_j} u_{jq} \quad \forall j \in \mathcal{J} \quad (12)$$

$$b_j \in \{0, 1\} \quad \forall j \in \mathcal{J}, \quad (13)$$

where \bar{C}_j denotes the bunkering capacity of port j , \bar{C}_j^{\min} and \bar{C}_j^{\max} are the minimum and maximum bunkering capacities at port j , respectively, the binary variable b_j equals 1 if bunkering port j is selected, u_{jq} is the amount of ammonia used for demand q , and $\bar{\mathcal{Q}}_j \subseteq \mathcal{Q}$ denotes the set of shipping demands that can be served by bunkering port j . Constraints (10) and (11) limit the bunkering capacity at each port, which in turn restricts the total amount of ammonia that is supplied to that port. Equations (12) balance the amounts of ammonia received and consumed at each bunkering port. Bunkering is typically classified as tank-to-ship or ship-to-ship; in this work, we assume ship-to-ship bunkering as it provides greater flexibility in terms of bunkering locations.

We impose some additional constraints on the amount of ammonia supplied by the bunkering ports to satisfy the fuel demand:

$$u_{jq} \leq \omega_q y_{jq} \quad \forall j \in \mathcal{J}, q \in \bar{\mathcal{Q}}_j \quad (14)$$

$$y_{jq} \leq b_j \quad \forall j \in \mathcal{J}, q \in \bar{\mathcal{Q}}_j \quad (15)$$

$$\sum_{q \in \mathcal{Q}} \sum_{j \in \bar{\mathcal{J}}_q} u_{jq} \geq \phi \sum_{q \in \mathcal{Q}} \gamma_q \quad (16)$$

$$y_{jq} \in \{0, 1\} \quad \forall j \in \mathcal{J}, q \in \bar{\mathcal{Q}}_j, \quad (17)$$

where the parameter ω_q denotes the maximum amount of ammonia that can be consumed by demand q from one bunkering port, and the binary variable y_{jq} equals 1 if demand q is served by bunkering port j , as indicated in constraints (14) and (15). Constraint (16) forces the total amount of ammonia supplied as marine fuel to be at least a given fraction, denoted by ϕ , of the total fuel demand.

The cost of ammonia production depends on the location and is a nonlinear function of the plant's capacity, which we approximate with a piecewise linear function modeled as follows:

$$C_{ih} = \sum_{l \in \mathcal{L}} [\lambda_{ihl} (\hat{C}_{i,l-1} - \hat{C}_{il}) + \hat{C}_{il} r_{ihl}] \quad \forall i \in \mathcal{I}, h \in \mathcal{H}_i \quad (18)$$

$$V_{ih}^{\text{plant}} = \sum_{l \in \mathcal{L}} [\lambda_{ihl} (\hat{V}_{i,l-1} - \hat{V}_{il}) + \hat{V}_{il} r_{ihl}] \quad \forall i \in \mathcal{I}, h \in \mathcal{H}_i \quad (19)$$

$$\lambda_{ihl} \leq r_{ihl} \quad \forall i \in \mathcal{I}, h \in \mathcal{H}_i, l \in \mathcal{L} \quad (20)$$

$$\sum_{l \in \mathcal{L}} r_{ihl} = p_{ih} \quad \forall i \in \mathcal{I}, h \in \mathcal{H}_i \quad (21)$$

$$r_{ihl} \in \{0, 1\} \quad \forall i \in \mathcal{I}, h \in \mathcal{H}_i, l \in \mathcal{L}, \quad (22)$$

where \mathcal{L} denotes the set of pieces chosen for the piecewise linear approximation, and the capacity-cost pair $(\hat{C}_{il}, \hat{V}_{il})$ is the point at the end of piece l . The binary variable r_{ihl} equals 1 if C_{ih} is within the range for piece l , and λ_{ihl} is a continuous variable between 0 and 1.

The electricity cost is determined separately from V_{ih}^{plant} . It is computed as follows:

$$V_{im}^{\text{elec}} = \mu_{im} E_{im} \quad \forall i \in \mathcal{I}, m \in \mathcal{M}_i, \quad (23)$$

where μ_{im} is the leveled cost of electricity (LCOE) at site i .

The capital cost for a bunkering port includes the costs of port construction or retrofit, bunker vessels, and ammonia storage tanks:

$$V_j^{\text{bunker}} = \delta_j b_j + \sigma_j N_j^{\text{vessel}} + \tau_j N_j^{\text{tank}} \quad \forall j \in \mathcal{J} \quad (24)$$

$$N_j^{\text{vessel}} \geq \alpha^{\text{vessel}} \bar{C}_j \quad \forall j \in \mathcal{J} \quad (25)$$

$$N_j^{\text{tank}} \geq \alpha^{\text{tank}} \bar{C}_j \quad \forall j \in \mathcal{J} \quad (26)$$

$$N_j^{\text{vessel}} \in \mathbb{Z}_+ \quad \forall j \in \mathcal{J} \quad (27)$$

$$N_j^{\text{tank}} \in \mathbb{Z}_+ \quad \forall j \in \mathcal{J}, \quad (28)$$

where δ_j , σ_j , and τ_j are cost parameters, and the required numbers of bunker vessels N_j^{vessel} and ammonia storage tanks N_j^{tank} are assumed to be proportional to the bunkering port capacity \bar{C}_j , determined using α^{vessel} and α^{tank} , which are the bunker speed and the ammonia tank capacity, respectively.

The ammonia transportation cost depends on the mode of transportation, which we preselect for every plant-port connection. We assume that pipelines are used if they can be built on land to connect the production plant and bunkering port; otherwise, ships are used for transporting the ammonia. For each plant-port pair, if a pipeline is selected as the transportation method, the associated edge (i, j) belongs to set $\mathcal{A}^{\text{pipe}}$; otherwise, it belongs to set $\mathcal{A}^{\text{ship}}$. The corresponding cost correlations are as follows:

$$V_{ij}^{\text{trans}} = \xi_{ij} x_{ij} + \beta_{ij} w_{ij} \quad \forall (i, j) \in \mathcal{A}^{\text{pipe}} \quad (29)$$

$$V_{ij}^{\text{trans}} = \zeta_{ij} x_{ij} + \eta_{ij} w_{ij} \quad \forall (i, j) \in \mathcal{A}^{\text{ship}} \quad (30)$$

with ξ_{ij} , β_{ij} , ζ_{ij} , and η_{ij} being the given cost parameters.

The costs are appropriately discounted based on the assumed discount rate and lifetimes of the capital investments; this means that in the typical case when we consider annual shipping demands, all costs are annualized. The overall optimization problem in the form of a mixed-integer linear program (MILP) is:

$$\begin{aligned} & \text{minimize} \quad \sum_{i \in I} \left(\sum_{h \in H_i} V_{ih}^{\text{plant}} + \sum_{m \in M_i} V_{im}^{\text{elec}} \right) + \sum_{j \in J} V_j^{\text{bunker}} + \sum_{i \in I} \sum_{j \in J} V_{ij}^{\text{trans}} \\ & \text{subject to} \quad (1)-(30). \end{aligned} \quad (31)$$

3.2. Data

In the following, we describe the data sources and methods used to determine the main parameter values for the proposed model. These include the shipping and fuel demands, the costs of renewable power generation, and the costs of green ammonia production and transportation.

3.2.1. Shipping and fuel demands

In this study, we consider 28 major container ship and dry bulk carrier routes that together account for about 23% of the global seaborne trade volume (Getting to Zero Coalition, 2021; UNCTAD, 2021). The shipping demands for these routes are shown in Table 1.

The key model parameter for each shipping demand q is the required amount of fuel γ_q , which is computed as follows:

$$\gamma_q = n_q^{\text{vessel}} d_q^{\text{vessel}} m_q^{\text{vessel}} \psi_q, \quad (32)$$

where n_q^{vessel} , d_q^{vessel} , m_q^{vessel} , and ψ_q denote the number of vessels required to meet shipping demand q , the distance traveled by each vessel, the vessel size in deadweight ton (DWT), and the unit ammonia fuel consumption in tonne per nautical mile per DWT, respectively. The total number of trips required to meet each shipping demand is calculated by dividing the trade volume by the vessel capacity. Here, the trade volume of a container ship is converted from TEUs (twenty-foot equivalent units) to tonnes assuming that 1 TEU holds 10 tonnes

of cargo. Assuming that all vessels of the same type have the same carrying capacity and travel at the same speed, we can estimate the time for completing one trip by dividing the travel distance by the ship speed and adding the average stay time at each port on the route. Given the total number of days per year that a vessel operates, we can compute how many trips one vessel can make every year; this then allows us to calculate n_q^{vessel} and d_q^{vessel} .

The main parameters used to determine the fuel demands are listed in Table 2, where the fuel consumption is given in heavy fuel oil (HFO) equivalent, which we convert to ammonia using a factor of 2.07. The ammonia fuel demands for the shipping routes are shown in Fig. 1, where the ports are depicted as red circles and the amount of ammonia required is indicated by the thickness of the blue lines. Also, we set the maximum amount of fuel that the fleet of ships for a given route can receive from one bunkering port to be the fuel tank capacity of a vessel multiplied by the number of vessels traveling on that route.

3.2.2. Renewable power generation

The renewable sources of energy considered in this study are solar and wind for which the availability and cost vary across different regions. We compute the LCOEs for solar and wind at each candidate plant location considering multiple factors, including solar irradiation, wind speed at 100 m height, average temperature, and water depth for offshore locations. We use the data from Hersbach et al. (2019) and present them in the form of heat maps in Fig. 2. We assume that both solar and wind can be used on land, whereas only wind is considered offshore. The water depth determines the type of offshore wind turbine that is used, with fixed-bottom wind turbines chosen for locations with water depths less than or equal to 60 m, and floating wind turbines required for locations with water depths greater than 60 m. Photovoltaic (PV) panel efficiency is affected by both solar irradiation and temperature; hence, we assume that PV panels can only be installed at locations where the annual average temperature is above 0 °C. We use LCOE data from NREL (2022) as a basis to estimate the LCOEs used in our study, which are shown in Fig. 3. NREL provides the LCOEs for various classes, categorized based on average solar irradiation and wind speed, as indicated by the dashed lines. The LCOE is constant for each class. To account for resource variability across different regions, we perform polynomial regression, taking into account the center point of each class, and use the resulting model to predict the LCOEs at all locations.

The maximum power generation capacity (or power potential) at each location depends on the solar irradiation and wind speed as well as the available land area at that location. Similar to how we estimate the LCOEs, we consider the capacity factor for each wind speed and solar irradiation range provided by NREL (2022), and apply polynomial regression to obtain capacity factors for all locations. In the case of solar energy, we assume that 2% of the land area can be used for PV panels and that they receive 10 h of sunlight per day. For wind farms, in addition to considering the required space between wind turbines, we assume that 5% of the land area can be used. The lower bounds we set on the generation capacities are realistic but not very restrictive. We assume a minimum PV farm capacity of 1 MW, which corresponds to the size of a typical community-scale PV farm. The minimum wind farm capacity is set to 250 kW, which is the capacity of a typical wind turbine. The power potential of each location is shown in Fig. 1.

3.2.3. Green ammonia production

The cost of producing green ammonia is dominated by the capital and electricity costs (Nayak-Luke and Bañares-Alcántara, 2020; Wang et al., 2021a). We consider the capital costs of the electrolyzer, air separation, and ammonia synthesis units. In the case of offshore production, we also account for the reverse osmosis unit and the construction of the offshore platform. We assume a 25-year lifetime for all units, with the exception of the electrolyzer, which is assumed to have a lifetime of 10 years. The cost parameters as well as the electricity

Table 1
Shipping routes considered in the study and the corresponding shipping demands.

Vessel type	Goods	Route	Trade volume (MTEU/yr)	Trade volume (Mt/yr)	Source
Container	-	Intra Asia	41.5	-	DHL (2022)
Container	-	Far East - North America	23.6	-	DHL (2022)
Container	-	Far East - Europe	14.7	-	DHL (2022)
Container	-	Far East - Latin America	6	-	DHL (2022)
Container	-	Europe - Far East	5.7	-	DHL (2022)
Container	-	Europe - North America	4.4	-	DHL (2022)
Container	-	North America - Far East	4.2	-	DHL (2022)
Container	-	Latin America - North America	2.9	-	DHL (2022)
Container	-	Europe - Latin America	1.8	-	DHL (2022)
Container	-	Latin America - Europe	1.8	-	DHL (2022)
Container	-	North America - Europe	1.7	-	DHL (2022)
Container	-	North America - Latin America	1.7	-	DHL (2022)
Container	-	Latin America - Far East	1.6	-	DHL (2022)
Dry bulk	Iron ore	Australia - China	-	689	Getting to Zero Coalition (2021)
Dry bulk	Iron ore	Brazil - China	-	270	Getting to Zero Coalition (2021)
Dry bulk	Iron ore	Australia - Japan	-	62	Getting to Zero Coalition (2021)
Dry bulk	Iron ore	Australia - South Korea	-	53	Getting to Zero Coalition (2021)
Dry bulk	Iron ore	Brazil - Malaysia	-	29	Getting to Zero Coalition (2021)
Dry bulk	Iron ore	South Africa - China	-	17	Getting to Zero Coalition (2021)
Dry bulk	Iron ore	Brazil - Japan	-	13	Getting to Zero Coalition (2021)
Dry bulk	Iron ore	Brazil - Netherlands	-	11	Getting to Zero Coalition (2021)
Dry bulk	Soy beans	United States - China	-	23	Getting to Zero Coalition (2021)
Dry bulk	Bauxite	Guinea - China	-	38	Getting to Zero Coalition (2021)
Dry bulk	Bauxite	Australia - China	-	31	Getting to Zero Coalition (2021)
Dry bulk	Manganese	South Africa - China	-	11	Getting to Zero Coalition (2021)
Dry bulk	Nickel ore	Philippines - China	-	25	Getting to Zero Coalition (2021)
Dry bulk	Nickel ore	Indonesia - China	-	18	Getting to Zero Coalition (2021)
Dry bulk	Forestry products	New Zealand - China	-	14	Getting to Zero Coalition (2021)

Table 2
Data used to determine the ammonia fuel demands (* values computed based on the 2018 data provided in the source).

Parameter	Unit	Bulk carrier	Container ship	Source
Vessel size	DWT	73,322	124,915	IMO (2020)*
HFO equivalent consumption	t/nm-DWT	2.53×10^{-6}	3.20×10^{-6}	IMO (2020)*
Speed-over-ground (SOG)	knots	11.19	14.25	IMO (2020)*
Days at sea	days/yr	202	228	IMO (2020)*
Fuel tank capacity	million gallons	0.8	3	Washington State Department of Ecology (1996)
Average port stay time	days	2.07	0.71	UNCTAD (2021)
HFO-to-NH ₃ conversion factor	t NH ₃ /t HFO	2.07	2.07	Getting to Zero Coalition (2021)

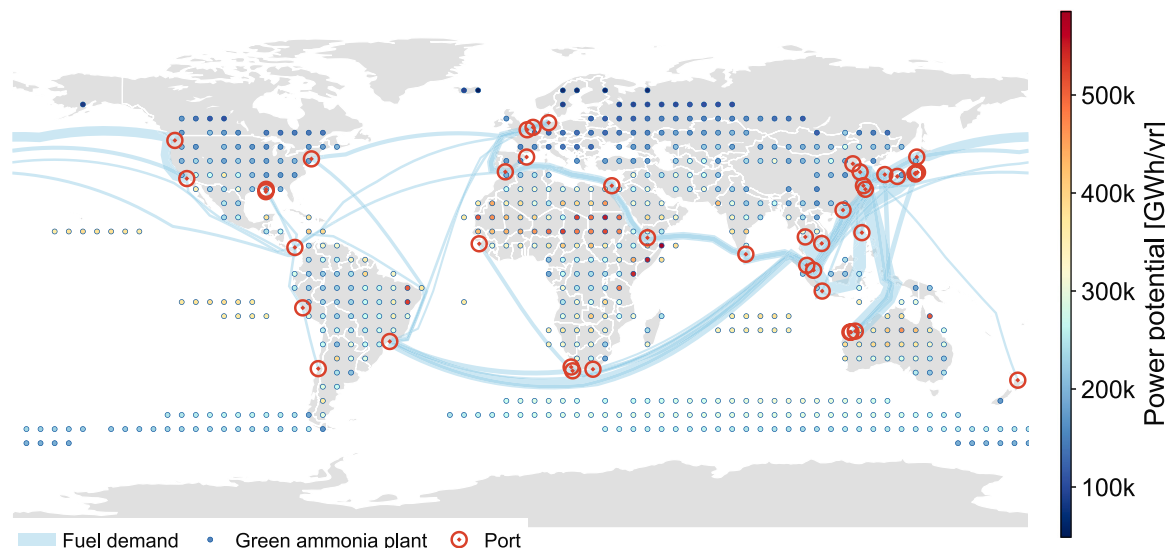


Fig. 1. Global map showing the 28 shipping routes, 42 ports, and 595 candidate ammonia production sites considered in this study. The thickness of each line indicates the amount of fuel required on the corresponding route.

consumption data are adopted from Wang et al. (2021a), where an electrolyzer efficiency of 54.3% (IEA, 2019) is assumed. To account for intermittency, we apply a capacity factor of 85% to the ammonia

synthesis and air separation processes based on results of our previous study (Wang et al., 2021a), while a conservative capacity factor of 30% is applied to the electrolyzer (Eichman et al., 2020). In our model, the

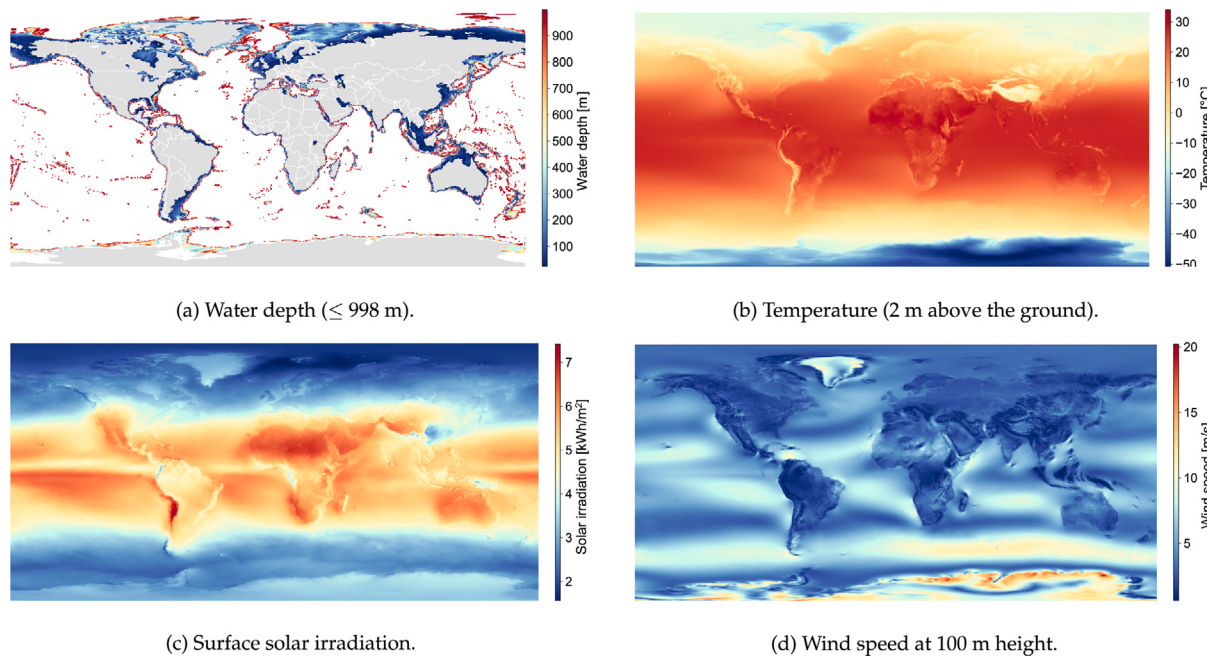


Fig. 2. Heat maps showing data averaged over years 2016–2020 (Hersbach et al., 2019).

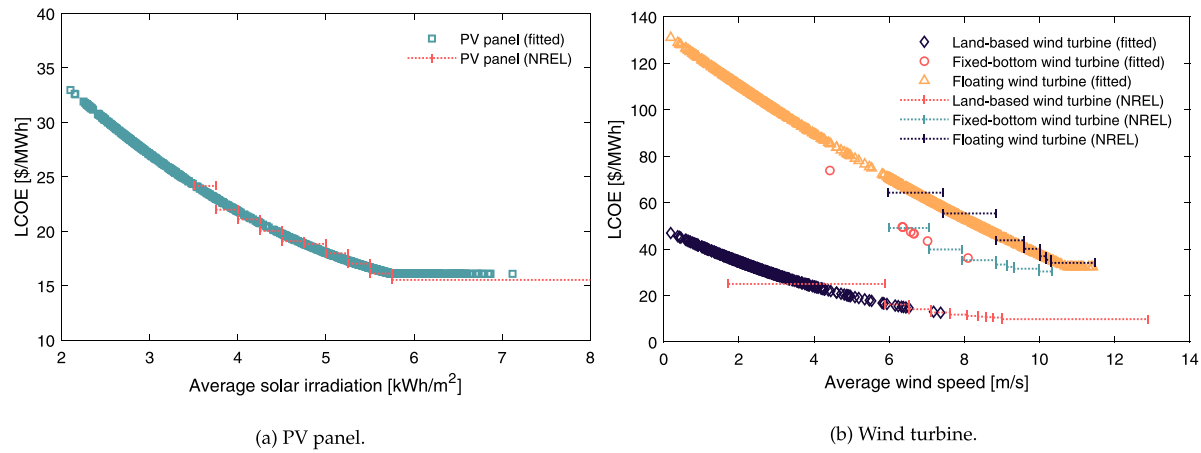


Fig. 3. LCOEs based on estimated 2050 cost (NREL, 2022) for all 595 candidate ammonia production locations compared to the NREL data.

nonlinear overall system capital cost is approximated with a piecewise linear function. We further assume that the storage cost is 5% of the ammonia production cost (excluding the electricity cost). We also consider other operating costs, although they are relatively small.

We place candidate ammonia production locations on a grid every 5° longitude and 5° latitude. We then filter out those locations with an LCOE greater than \$50/MWh and offshore locations with a known water depth greater than 998 m, after which we arrive at the 595 candidate locations shown in Fig. 1.

3.2.4. Ammonia transportation

For transporting ammonia on land, we consider pipelines at a cost of \$1.616/t-100 km (George Thomas, 2006). When it needs to be shipped across water, we consider tanker ships chartered at a cost of \$7.5/t and \$0.375/t-100 km (Salmon and Bañares-Alcántara, 2021). The shortest distance between two locations is calculated using the haversine formula; to obtain a better estimate of the actual distance for transportation, we further multiply the computed distance by a factor of 1.1 in the case of a pipeline and 2.0 for shipping.

4. Results and discussion

Using the proposed optimization model, we design a global network of green ammonia production plants, transportation links, and bunkering ports that satisfy the shipping demands shown in Fig. 1. All model instances were implemented in Julia v1.7.3 using the mathematical optimization modeling environment JuMP v1.1.0 (Dunning et al., 2017) and solved using Gurobi v9.0.0.

4.1. Base case

We first solve the base case in which all of the considered marine fuel demand is met with green ammonia. The optimal solution is shown in Fig. 4, where the selected ammonia production plants are shown as yellow filled circles, the selected bunkering ports are shown as dotted red circles, each square represents a PV farm, and each cross represents a wind farm. The capacities are indicated by the sizes of the markers while the color of the PV and wind farm markers depicts the local LCOE. The amount of green ammonia fuel consumed on each shipping route is indicated by the thickness of the solid light-blue line for that

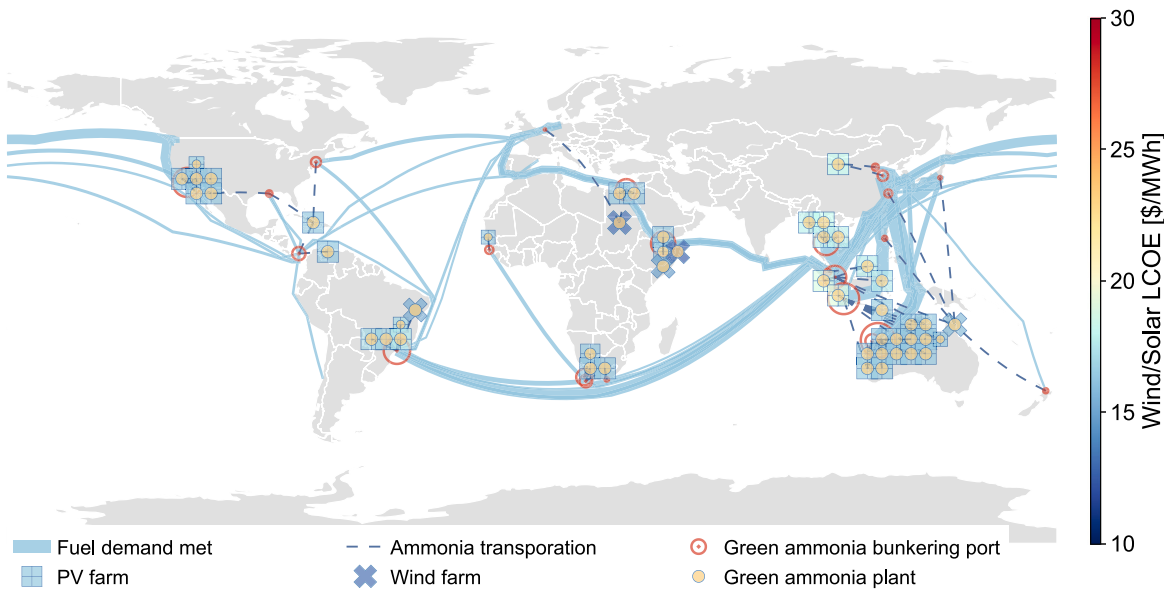


Fig. 4. Optimal network design for the base case (100% fuel demand met). Capacities are represented by the marker sizes, and the color of the PV and wind farm markers indicates the local LCOE.

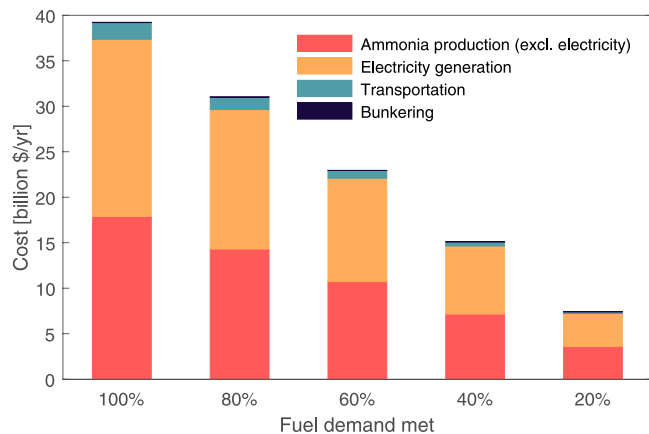


Fig. 5. Cost breakdowns for different ammonia fuel demand scenarios.

route, and the dashed lines represent ammonia transportation from production sites to bunkering ports.

To meet all fuel demand, 115 Gt of green ammonia is produced, using 1,065 GW of solar-based and 128 GW of wind-based electricity. The amount of solar-based electricity is almost an order of magnitude larger compared to wind-based electricity as the LCOE for solar is lower in most regions, except for a few locations in the Middle East, Australia, and South America. Fig. 5 shows the cost breakdown (the base case corresponds to the case with 100% fuel demand met), where the ammonia production and electricity generation costs dominate, accounting for 45% and 50% of the total cost, respectively. The transportation cost accounts for about 5% of the total cost, while the cost for the bunkering infrastructure, which only involves retrofitting existing ports, is almost negligible compared to the other costs.

Green ammonia production is concentrated in Australia, North America, South America, Africa, and around the Mediterranean and Red Sea regions. These regions exhibit low electricity costs and are typically located near ports that connect trade routes with significant fuel demands. One can observe long-distance transportation of ammonia from Australia to ports in New Zealand and several Asian countries, as well as from Sudan to Europe. The reason is that both Asia and

Europe have dense trade channels and hence high fuel demands yet the renewable electricity costs in those regions are relatively high (see power potential shown in Fig. 1). Since ammonia transportation costs are relatively low compared to ammonia production costs, the best strategy seems to be to produce ammonia at low-cost locations and then transport it to large ports. Another reason for no ammonia production plants being selected in Europe is that there are ports (e.g. Port of Aden and Suez Port) with access to cheap ammonia along most shipping routes that are connected to Europe.

4.2. Solutions for varying ammonia demands

We investigate how the solution changes depending on the fuel demand satisfaction target that we set in the model. Fig. 5 shows the cost breakdowns for, in addition to the base case, the cases in which we require 80%, 60%, 40%, and 20% of the total fuel demand to be met with green ammonia. There is no notable change in the cost structure across the different scenarios. However, the cost per unit of ammonia used as marine fuel (from production to consumption) decreases from \$341/t in the base case to \$323/t in the 20% demand satisfaction case, indicating that increasingly expensive production locations need to be used as the ammonia demand increases.

Fig. 6 shows the optimal network designs in the 20% and 60% demand scenarios; the results for all considered demand scenarios are provided in the supplementary material. In the 20% case, the following green corridors are selected: between Europe and the Far East, from Australia to China, and from the Far East to North America. The largest ammonia production sites and bunkering ports are established in Africa, along the shipping route connecting Europe and Asia via the Suez Canal and the Gulf of Aden, which are near the region with the lowest electricity cost. For the container ship route connecting the Far East to North America, the ammonia plants are constructed in the U.S., specifically in California and Arizona, which have abundant solar energy. The Australia–China iron ore route is one of the busiest trade routes, and it is supplied with green ammonia produced at low cost in Australia, which is in line with Australia's recent investment in green hydrogen and ammonia production.

When we aim to satisfy 60% of the fuel demand with green ammonia, 21 of the 28 shipping routes are chosen along with 15 bunkering ports and 31 green ammonia plants (see Fig. 6b). Most ammonia plants are located in Africa, Australia, and North America. Compared to the

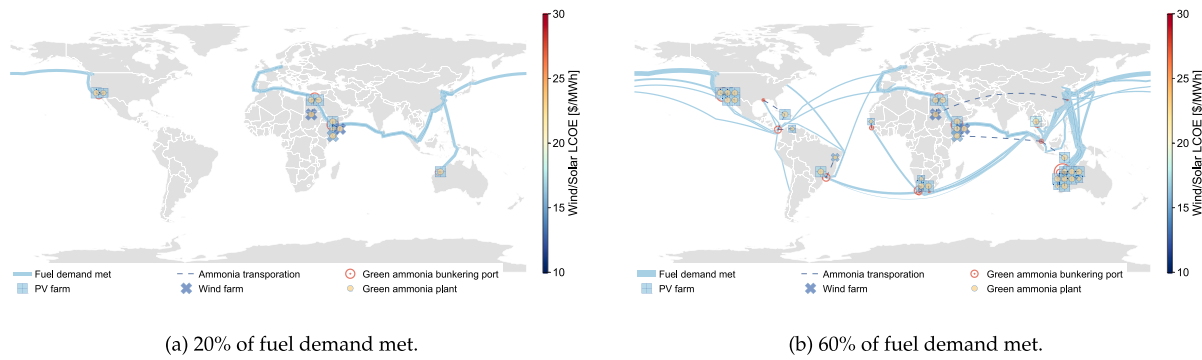


Fig. 6. Optimal network designs in the 20% and 60% fuel demand satisfaction cases.

20% case, the ammonia production in Australia is significantly higher. Only two plants are located in the Far East region, one in Thailand and one in Indonesia; this is in contrast to the base case where ten ammonia plants are placed in that region. This is due to the large fuel demand on the Intra Asia route, which can be mostly met using ammonia produced in Australia in the 60% case, but to satisfy 100% of the fuel demand, additional ammonia supply from Asia is needed.

4.3. Production–transportation trade-off

As already observed in the base case, there is a clear trade-off between ammonia production and transportation costs, which our model optimizes to obtain the best network design. Here, we investigate this trade-off further by examining the solutions for varying transportation costs. To this end, we introduce a transportation cost factor (TCF) with which the total transportation cost is multiplied in the model, i.e. the TCF is 1 in the base case. We vary the TCF between 0.1 and 9 and summarize the results in Fig. 7, which shows the total amount of ammonia transported in mt-km and the total ammonia production cost (including electricity cost) as functions of the TCF. The amount of ammonia transported decreases as the transportation cost increases and plateaus when the TCF exceeds 5. In contrast, the cost of ammonia production increases with the transportation cost since, to reduce the need of transportation, the solution suggests selecting plants that are closer to the ports but have higher production costs. Several notable structural changes in the network can be observed as the transportation cost changes. For instance, when the TCF is increased to 2, we see that long-distance transportation from Australia to East Asia is replaced by local ammonia production in East Asia. Also, when the TCF is set to 7, we start seeing ammonia being produced in Europe. The network designs for all considered TCFs can be found in the supplementary material.

4.4. Impact of local reduction in ammonia production cost

Since ammonia production, including electricity generation, is by far the largest cost contributor, we expect that significant local reduction in ammonia production cost can give those locations a considerable competitive advantage in a future green ammonia fuel market. We use the U.S. as an example to verify this hypothesis. This is motivated by the U.S.’s Inflation Reduction Act (IRA), which was signed into law in August 2022. One of the IRA’s main objectives is to reduce GHG emissions by providing tax incentives to industries and individuals for implementing low-carbon technologies such as renewable electricity generation and clean fuel production (U.S. Government Publishing Office, 2022). With those tax incentives, optimistic (but not unrealistic) estimates predict that the green ammonia production cost could be reduced to as low as \$255/t. Compared to the average ammonia production cost of \$325/t in our base case, this huge cost reduction could be a real game changer for the U.S. green ammonia industry.

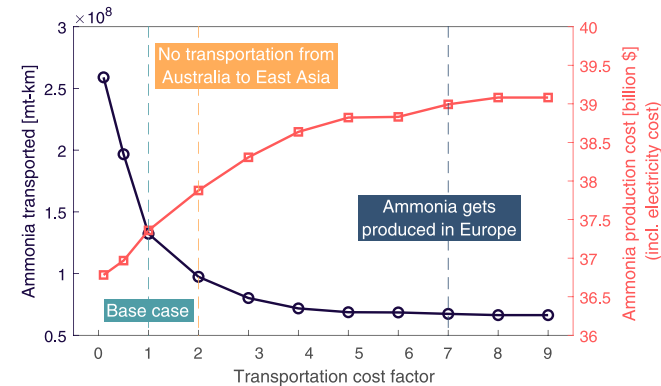


Fig. 7. Amounts of ammonia transported and ammonia production costs for different TCFs.

In our analysis, we study the changes in the network design as we vary the ammonia production (including electricity generation) cost reduction from 5% to 20%. Fig. 8 shows the network designs for the 5% and 20% cases (another 10% case is shown in the supplementary material). When the U.S. ammonia production cost decreases by 5%, the amount of green ammonia produced in the U.S. increases by more than 70% compared to the base case, reaching a production capacity of 14,822 kt. While a significant amount of ammonia is produced in Mexico in the base case, that capacity is now located in the U.S. in the 5% cost reduction case. When the ammonia production cost is reduced by 20%, the U.S. ammonia production capacity increases to 32,850 kt. In that case, the U.S. does not only produce enough to meet its local demand but also exports green ammonia to other regions, namely Europe, China, and Japan.

4.5. Comparison with single-corridor optimization

To demonstrate the value of our global network analysis, we compare the proposed network design with green corridor designs obtained from considering each shipping route individually. Fig. 9 shows two examples of green corridor designs obtained from single-corridor optimization. Here, the fuel demands of the individual Brazil-to-China and Intra-Asia routes are met by ammonia transported from Africa to China and from Africa to Singapore, respectively, clearly due to the low electricity cost in Africa. However, neither of these two ammonia transportation links is included in the optimal network design obtained from the global analysis (see Fig. 4). Our holistic optimization considering all shipping routes simultaneously finds that it is more cost-efficient to use the ammonia produced in Africa to satisfy demands at more nearby locations. As the maximum production capacity is reached in Africa, more ammonia is directly produced in Asia to meet fuel demands in that region. This comparison shows that the global network optimization

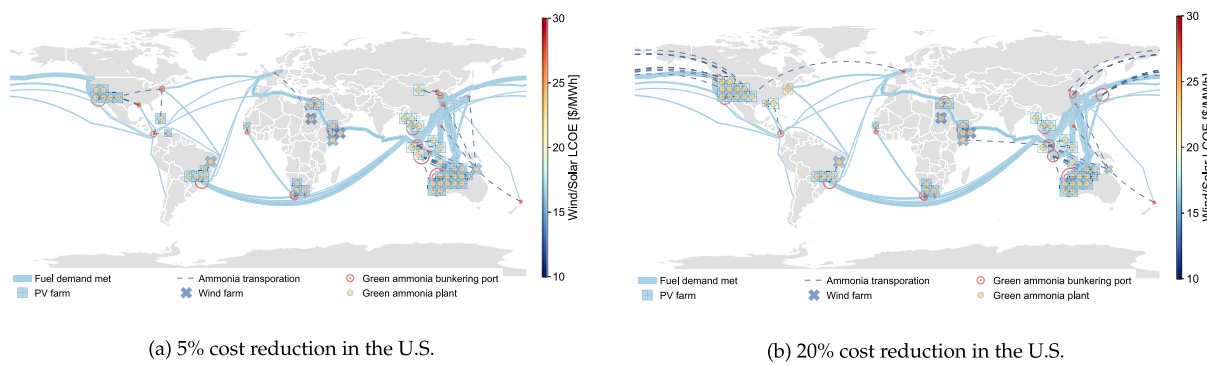


Fig. 8. Optimal network designs for U.S. ammonia production cost reduction of 5% and 20%.

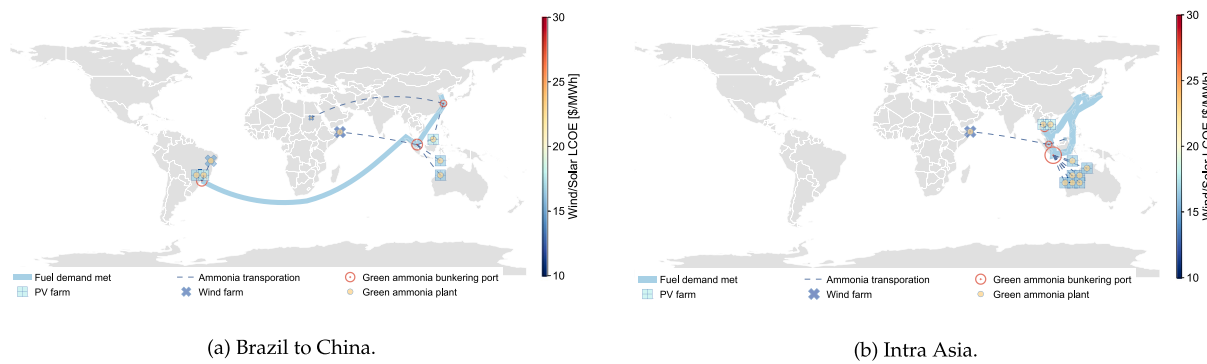


Fig. 9. Optimal corridor designs from single-corridor optimization for two selected routes.

can better capture the synergies and trade-offs across different shipping routes and geographical regions, which demonstrates the value of our study. Finally, the results from all 28 single-corridor optimization runs can be found in the supplementary material.

5. Conclusions

In this work, we conducted a global analysis of green shipping corridors by designing a network of alternative fuel production sites, transportation links, and bunkering ports that can meet the fuel demand of 28 major shipping routes that together account for about 23% of the global seaborne trade volume. Our alternative marine fuel of choice was green ammonia produced using solar- or wind-based electricity. The study considered 595 candidate ammonia production sites, both onshore and offshore, and 42 major ports that can be retrofitted for ammonia bunkering. An MILP supply chain design model, which integrates a facility location formulation and a flow-capturing location formulation, was used to obtain the optimal network design.

Assuming estimated technology costs for 2050, the solution for our base case indicates that 115 Gt of green ammonia is required to meet all considered fuel demand, which can be provided at a minimum cost of \$341/t (includes production and distribution). The optimal network design suggests to manufacture the ammonia primarily in Australia, North America, South America, Africa, and in the Mediterranean and Red Sea regions, which all exhibit low renewable electricity costs and are close to major ports. Some long-distance transportation of ammonia from production sites to bunkering ports is also proposed, indicating a clear trade-off between production and transportation costs, which we further investigated in a sensitivity analysis. In another analysis, we examined the impact of local ammonia production cost reduction on the network design using the U.S. as an example (inspired by the recent Inflation Reduction Act). The results highlight the clear competitive advantage that such cost reductions can provide in a future green ammonia market, to an extent that ammonia is not only produced to meet local demand but also exported to other countries.

The concept of green shipping corridors has only emerged in the past few years, and so far, systematic analyses have only been provided for individual shipping routes. However, global network analyses that simultaneously consider many shipping routes, like we did here, are required to capture the potential synergies and trade-offs across different routes and regions, which we also demonstrate in our study. The proposed model can be readily applied to consider other alternative marine fuels, such as LNG and methanol, and more shipping routes, e.g. by also including liner ships. As such, it could serve as a valuable decision-support tool for governments and other organizations that want to promote the development of green shipping corridors.

Declaration of competing interest

The authors declare that they have no known competing financial interests or personal relationships that could have appeared to influence the work reported in this paper.

Acknowledgments

This work was supported in part by the State of Minnesota, United States through an appropriation from the Renewable Development Account to the University of Minnesota West Central Research and Outreach Center. H.W. further acknowledges financial support through a UMII MnDRIVE Graduate Assistantship from the University of Minnesota, United States.

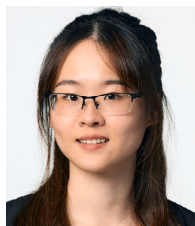
Appendix A. Supplementary data

Supplementary material related to this article can be found online at <https://doi.org/10.1016/j.dche.2022.100082>.

References

- Adli, Nadia Mohd, Zhang, Hao, Mukherjee, Shreya, Wu, Gang, 2018. Review—ammonia oxidation electrocatalysis for hydrogen generation and fuel cells. *J. Electrochem. Soc.* 165 (15), J3130–J3147. <http://dx.doi.org/10.1149/2.0191815jes>.
- Al-Aboosi, Fadhl Y., El-Halwagi, Mahmoud M., Moore, Margaux, Nielsen, Rasmus B., 2021. Renewable ammonia as an alternative fuel for the shipping industry. *Curr. Opin. Chem. Eng.* 31, 100670. <http://dx.doi.org/10.1016/j.coche.2021.100670>.
- Allman, Andrew, Daoutidis, Prodromos, Tiffany, Douglas, Kelley, Stephen, 2017. A framework for ammonia supply chain optimization incorporating conventional and renewable generation. *AIChE J.* 63 (10), 4390–4402. <http://dx.doi.org/10.1002/aic.15838>.
- Allman, Andrew, Palys, Matthew J., Daoutidis, Prodromos, 2019. Scheduling-informed optimal design of systems with time-varying operation: A wind-powered ammonia case study. *AIChE J.* 65 (7), e16434. <http://dx.doi.org/10.1002/aic.16434>.
- Alvarez, Jose A. Lopez, Buijs, Paul, Deluster, Rogier, Coelho, Leandro C., Ur-savas, Evrim, 2020. Strategic and operational decision-making in expanding supply chains for LNG as a fuel. *Omega* 97, 102093. <http://dx.doi.org/10.1016/j.omega.2019.07.009>.
- Arslan, Okan, Karaşan, Oya Ekin, Mahjoub, A. Ridha, Yaman, Hande, 2019. A branch-and-cut algorithm for the alternative fuel refueling station location problem with routing. *Transp. Sci.* 53 (4), 1107–1125. <http://dx.doi.org/10.1287/trsc.2018.0869>.
- Baltrusaitis, Jonas, 2017. Sustainable ammonia production. *ACS Sustain. Chem. Eng.* 5 (11), 9527. <http://dx.doi.org/10.1021/acssuschemeng.7b03719>.
- Bapna, Ravi, Thakur, Lakshman S., Nair, Suresh K., 2002. Infrastructure development for conversion to environmentally friendly fuel. *European J. Oper. Res.* 142 (3), 480–496. [http://dx.doi.org/10.1016/S0377-2217\(01\)00309-5](http://dx.doi.org/10.1016/S0377-2217(01)00309-5).
- Beerbühl, S. Schulte, Fröhling, Magnus, Schultmann, Frank, 2015. Combined scheduling and capacity planning of electricity-based ammonia production to integrate renewable energies. *European J. Oper. Res.* 241 (3), 851–862. <http://dx.doi.org/10.1016/j.ejor.2014.08.039>.
- Berman, Oded, Larson, Richard C., Fouska, Nikoletta, 1992. Optimal location of discretionary service facilities. *Transp. Sci.* 26 (3), 201–211. <http://dx.doi.org/10.1287/trsc.26.3.201>.
- Bittante, A., Pettersson, F., Saxén, H., 2018. Optimization of a small-scale LNG supply chain. *Energy* 148, 79–89. <http://dx.doi.org/10.1016/j.energy.2018.01.120>.
- Cardoso, João Sousa, Silva, Valter, Rocha, Rodolfo C., Hall, Matthew J., Costa, Mário, Eusébio, Daniela, 2021. Ammonia as an energy vector: Current and future prospects for low-carbon fuel applications in internal combustion engines. *J. Clean. Prod.* 296, 126562. <http://dx.doi.org/10.1016/j.jclepro.2021.126562>.
- Cesaro, Zac, Ives, Matthew, Nayak-Luke, Richard, Mason, Mike, Bañares-Alcántara, René, 2021. Ammonia to power: Forecasting the leveled cost of electricity from green ammonia in large-scale power plants. *Appl. Energy* 282, 116009. <http://dx.doi.org/10.1016/j.apenergy.2020.116009>.
- Demirhan, C. Doga, Tso, William W., Powell, Joseph B., Pistikopoulos, Efstratios N., 2019. Sustainable ammonia production through process synthesis and global optimization. *AIChE J.* 65 (7), e16498. <http://dx.doi.org/10.1002/aic.16498>.
- DHL, 2022. Ocean freight market update - February 2022. Technical report, URL <https://lot.dhl.com/dhl-ocean-freight-market-update-february-2022/>.
- Doymus, Mehmet, Denktaş Sakar, Gul, Topaloglu Yıldız, Seyda, Acık, Abdullah, 2022. Small-scale LNG supply chain optimization for LNG bunkering in Turkey. *Comput. Chem. Eng.* 162, 107789. <http://dx.doi.org/10.1016/j.compchemeng.2022.107789>.
- Dunning, Iain, Huchette, Joey, Lubin, Miles, 2017. JuMP: A modeling language for mathematical optimization. *SIAM Rev.* 59 (2), 295–320. <http://dx.doi.org/10.1137/15M1020575>.
- Eichman, Josh, Koleva, Mariya, Guerra, Omar J., McLaughlin, Brady, 2020. Optimizing an integrated renewable electrolysis system. Technical report, URL <https://www.nrel.gov/docs/fy20osti/75635.pdf>.
- Erdemir, Dogan, Dincer, Ibrahim, 2021. A perspective on the use of ammonia as a clean fuel: Challenges and solutions. *Int. J. Energy Res.* 45 (4), 4827–4834. <http://dx.doi.org/10.1002/er.6232>.
- George Thomas, George Parks, 2006. Potential roles of ammonia in a hydrogen economy—a study of issues related to the use ammonia for on-board vehicular hydrogen storage. Technical report, URL https://www.energy.gov/sites/prod/files/2015/01/f19/fcto_nh3_h2_storage_white_paper_2006.pdf.
- Getting to Zero Coalition, 2021. The next wave: Green corridors. a special report for the getting to zero coalition. Technical report, URL <https://www.globalmaritimeforum.org/content/2021/11/The-Next-Wave-Green-Corridors.pdf>.
- Hansson, Julia, Brynolf, Selma, Fridell, Erik, Lehtveer, Mariliis, 2020. The potential role of ammonia as marine fuel-based on energy systems modeling and multi-criteria decision analysis. *Sustainability* 12 (8), 3265. <http://dx.doi.org/10.3390/su12083265>.
- Hersbach, H., Bell, B., Berrisford, P., Biavati, G., Horányi, A., Muñoz Sabater, J., Nicolas, J., Peuebey, C., Radu, R., Rozum, I., Schepers, D., Simmons, A., Soci, C., Dee, D., Thépaut, J.-N., 2019. ERA5 monthly averaged data on single levels from 1959 to present. <http://dx.doi.org/10.24381/cds.f17050d7>, Accessed on 08-30-2022.
- Hodgson, M. John, 1990. A flow-capturing location-allocation model. *Geogr. Anal.* 22 (3), 270–279. <http://dx.doi.org/10.1111/j.1538-4632.1990.tb00210.x>.
- Honma, Yudai, Kuby, Michael, 2019. Node-based vs. path-based location models for urban hydrogen refueling stations: Comparing convenience and coverage abilities. *Int. J. Hydrogen Energy* 44 (29), 15246–15261. <http://dx.doi.org/10.1016/j.ijhydene.2019.03.262>.
- IEA, 2019. The future of hydrogen - seizing today's opportunities. Technical report, URL https://iea.blob.core.windows.net/assets/9e3a3493-b9a6-4b7d-b499-7ca48e357561/The_Future_of_Hydrogen.pdf.
- IMO, 2018. Adoption of the initial IMO strategy on reduction of GHG emissions from ships and existing IMO activity related to reducing GHG emissions in the shipping sector. Technical report, IMO London, URL https://unfccc.int/sites/default/files/resource/250 IMO%20submission_Talanoa%20Dialogue_April%202018.pdf.
- IMO, 2020. Fourth greenhouse gas study 2020. Technical report, URL <https://www.imo.org/en/OurWork/Environment/Pages/Fourth-IMO-Greenhouse-Gas-Study-2020.aspx>.
- IRENA, AEA, 2022. Innovation outlook: Renewable ammonia. Technical report, International Renewable Energy Agency, Ammonia Energy Association, ISBN: 978-92-9260-423-3, URL <https://www.irena.org/publications/2022/May/Innovation-Outlook-Renewable-Ammonia>.
- Jeerh, Georgina, Zhang, Mengfei, Tao, Shanwen, 2021. Recent progress in ammonia fuel cells and their potential applications. *J. Mater. Chem. A* 9, 727–752. <http://dx.doi.org/10.1039/DOTA08810B>.
- Jokinen, Raine, Pettersson, Frank, Saxén, Henrik, 2015. An MILP model for optimization of a small-scale LNG supply chain along a coastline. *Appl. Energy* 138, 423–431. <http://dx.doi.org/10.1016/j.apenergy.2014.10.039>.
- Kim, Jong-Geun, Kuby, Michael, 2012. The deviation-flow refueling location model for optimizing a network of refueling stations. *Int. J. Hydrogen Energy* 37 (6), 5406–5420. <http://dx.doi.org/10.1016/j.ijhydene.2011.08.108>.
- Kuby, Michael, Lim, Seow, 2005. The flow-refueling location problem for alternative-fuel vehicles. *Socio-Econ. Plan. Sci.* 39 (2), 125–145. <http://dx.doi.org/10.1016/j.seps.2004.03.001>.
- MacFarlane, Douglas R., Cherepanov, Pavel V., Choi, Jaecheol, Suryanto, Bryan H.R., Hodgetts, Rebecca Y., Bakker, Jacinta M., Vallana, Federico M., Ferrero, Simonov, Alexandr N., 2020. A roadmap to the ammonia economy. *Joule* 4 (6), 1186–1205. <http://dx.doi.org/10.1016/j.joule.2020.04.004>.
- Nayak-Luke, Richard Michael, Bañares-Alcántara, René, 2020. Techno-economic viability of islanded green ammonia as a carbon-free energy vector and as a substitute for conventional production. *Energy Environ. Sci.* 13, 2957–2966. <http://dx.doi.org/10.1039/D0EE01707H>.
- NREL, 2022. Electricity annual technology baseline (ATB) data download. URL <https://atb.nrel.gov/electricity/2022/data>, Accessed on 10-05-2022.
- Obara, Shin'ya, 2019. Energy and exergy flows of a hydrogen supply chain with truck transportation of ammonia or methyl cyclohexane. *Energy* 174, 848–860. <http://dx.doi.org/10.1016/j.energy.2019.01.103>.
- Ogumerem, Gerald S., Tso, William W., Demirhan, C. Doga, Lee, Seung Y., Song, Han E., Pistikopoulos, Efstratios N., 2019. Toward the optimization of hydrogen, ammonia, and methanol supply chains. *IFAC-PapersOnLine* 52 (1), 844–849. <http://dx.doi.org/10.1016/j.ifacol.2019.06.167>.
- Palys, Matthew J., Allman, Andrew, Daoutidis, Prodromos, 2019a. Exploring the benefits of modular renewable-powered ammonia production: A supply chain optimization study. *Ind. Eng. Chem. Res.* 58 (15), 5898–5908. <http://dx.doi.org/10.1021/acs.iecr.8b04189>.
- Palys, Matthew J., Daoutidis, Prodromos, 2020. Using hydrogen and ammonia for renewable energy storage: A geographically comprehensive techno-economic study. *Comput. Chem. Eng.* 136, 106785. <http://dx.doi.org/10.1016/j.compchemeng.2020.106785>.
- Palys, Matthew J., Kuznetsov, Anatoliy, Tallaksen, Joel, Reese, Michael, Daoutidis, Prodromos, 2019b. A novel system for ammonia-based sustainable energy and agriculture: Concept and design optimization. *Chem. Eng. Process.-Process Intensif.* 140, 11–21. <http://dx.doi.org/10.1016/j.cep.2019.04.005>.
- Palys, Matthew J., McCormick, Alon, Cussler, E.L., Daoutidis, Prodromos, 2018. Modeling and optimal design of absorbent enhanced ammonia synthesis. *Processes* 6 (7), 91. <http://dx.doi.org/10.3390/pr6070091>.
- Palys, Matthew J., Wang, Hanchu, Zhang, Qi, Daoutidis, Prodromos, 2021. Renewable ammonia for sustainable energy and agriculture: vision and systems engineering opportunities. *Curr. Opin. Chem. Eng.* 31, 100667. <http://dx.doi.org/10.1016/j.coche.2020.100667>.
- Prevljak, Naida Hakirevic, 2022. World's first ammonia-ready vessel delivered. Accessed on 08-30-2022. <https://www.offshore-energy.biz/worlds-first-ammonia-ready-vessel-delivered/>.
- Reese, Michael, Marquart, Cory, Malmali, Mahdi, Wagner, Kevin, Buchanan, Eric, McCormick, Alon, Cussler, Edward L., 2016. Performance of a small-scale haber process. *Ind. Eng. Chem. Res.* 55 (13), 3742–3750. <http://dx.doi.org/10.1021/acs.iecr.5b04909>.
- Salmon, Nicholas, Bañares-Alcántara, René, 2021. Green ammonia as a spatial energy vector: a review. *Sustain. Energy Fuels* 5 (11), 2814–2839. <http://dx.doi.org/10.1039/DSE00345C>.
- Salmon, Nicholas, Bañares-Alcántara, René, Nayak-Luke, Richard, 2021. Optimization of green ammonia distribution systems for intercontinental energy transport. *Iscience* 24 (8), 102903. <http://dx.doi.org/10.1016/j.isci.2021.102903>.

- Sánchez, Antonio, Castellano, Elena, Martín, Mariano, Vega, Pastora, 2021a. Evaluating ammonia as green fuel for power generation: A thermo-chemical perspective. *Appl. Energy* 293, 116956. <http://dx.doi.org/10.1016/j.apenergy.2021.116956>.
- Sánchez, Antonio, Martín, Mariano, 2018. Optimal renewable production of ammonia from water and air. *J. Clean. Prod.* 178, 325–342. <http://dx.doi.org/10.1016/j.jclepro.2017.12.279>.
- Sánchez, Antonio, Martín, Mariano, Zhang, Qi, 2021b. Optimal design of sustainable power-to-fuels supply chains for seasonal energy storage. *Energy* 234, 121300. <http://dx.doi.org/10.1016/j.energy.2021.121300>.
- Shukla, Aviral, Pekny, Joseph, Venkatasubramanian, Venkat, 2011. An optimization framework for cost effective design of refueling station infrastructure for alternative fuel vehicles. *Comput. Chem. Eng.* 35 (8), 1431–1438. <http://dx.doi.org/10.1016/j.compchemeng.2011.03.018>.
- Tang, Jianping, Kang, Lixia, Liu, Yongzhong, 2022. Design and optimization of a clean ammonia synthesis system based on biomass gasification coupled with a Ca–Cu chemical loop. *Ind. Eng. Chem. Res.* <https://doi.org/10.1012/acs.iecr.2c00616>.
- Tragantalerksak, Suda, Holt, John, Rönnqvist, Mikael, 2000. An exact method for the two-echelon, single-source, capacitated facility location problem. *European J. Oper. Res.* 123 (3), 473–489. [http://dx.doi.org/10.1016/S0377-2217\(99\)00105-8](http://dx.doi.org/10.1016/S0377-2217(99)00105-8).
- UNCTAD, 2018. Review of maritime transport 2018. Technical report, URL https://unctad.org/system/files/official-document/rmt2018_en.pdf.
- UNCTAD, 2021. Review of maritime transport 2021. Technical report, URL https://unctad.org/system/files/official-document/rmt2021_en_0.pdf.
- Ursavas, Evrin, Zhu, Stuart X., Savelsbergh, Martin, 2020. LNG bunkering network design in inland waterways. *Transp. Res. C* 120, 102779. <http://dx.doi.org/10.1016/j.trc.2020.102779>.
- U.S. Department of State, 2022. Green shipping corridors framework. URL <https://www.state.gov/green-shipping-corridors-framework/>, accessed: 08/31/2022.
- U.S. Government Publishing Office, 2022. H.R.5376 - Inflation Reduction Act of 2022. URL <https://www.congress.gov/bill/117th-congress/house-bill/5376/text>.
- Wang, Ying-Wei, 2007. An optimal location choice model for recreation-oriented scooter recharge stations. *Transp. Res. D* 12 (3), 231–237. <http://dx.doi.org/10.1016/j.trd.2007.02.002>.
- Wang, Hanchu, Daoutidis, Prodromos, Zhang, Qi, 2021a. Harnessing the wind power of the ocean with green offshore ammonia. *ACS Sustain. Chem. Eng.* 9 (43), 14605–14617. <http://dx.doi.org/10.1021/acssuschemeng.1c06030>.
- Wang, Ganzhou, Mitsos, Alexander, Marquardt, Wolfgang, 2017. Conceptual design of ammonia-based energy storage system: System design and time-invariant performance. *AIChE J.* 63 (5), 1620–1637. <http://dx.doi.org/10.1002/aic.15660>.
- Wang, Ganzhou, Mitsos, Alexander, Marquardt, Wolfgang, 2020. Renewable production of ammonia and nitric acid. *AIChE J.* 66 (6), e16947. <http://dx.doi.org/10.1002/aic.16947>.
- Wang, Hanchu, Palys, Matthew, Daoutidis, Prodromos, Zhang, Qi, 2021b. Optimal design of sustainable ammonia-based food-energy-water systems with nitrogen management. *ACS Sustain. Chem. Eng.* 9 (7), 2816–2834. <http://dx.doi.org/10.1021/acssuschemeng.0c08643>.
- Wang, Lu, Xia, Meikun, Wang, Hong, Huang, Kefeng, Qian, Chenxi, Maravelias, Christos T., Ozin, Geoffrey A., 2018. Greening ammonia toward the solar ammonia refinery. *Joule* 2 (6), 1055–1074. <http://dx.doi.org/10.1016/j.joule.2018.04.017>.
- Washington State Department of Ecology, 1996. Guidelines for determining oil spill volume in the field. Technical report, URL <https://apps.ecology.wa.gov/publications/documents/96250.pdf>.
- Wojciech, Adam, Middleton, Hugh, Damopoulos, Ioannis, Van herle, Jan, 2003. Ammonia as a fuel in solid oxide fuel cells. *J. Power Sources* 118 (1), 342–348. [http://dx.doi.org/10.1016/S0378-7753\(03\)00083-1](http://dx.doi.org/10.1016/S0378-7753(03)00083-1).
- Zhang, Hanfei, Wang, Ligang, Maréchal, François, Desideri, Umberto, et al., 2020. Techno-economic comparison of green ammonia production processes. *Appl. Energy* 259, 114135. <http://dx.doi.org/10.1016/j.apenergy.2019.114135>.



Hanchu Wang is a graduate research assistant and currently pursuing her Ph.D. in the Department of Chemical Engineering and Materials Science at the University of Minnesota. She obtained B.S. degrees in Chemical Engineering and Mathematics from the University of Maryland, College Park in 2018. Her research focuses on the system-level analysis and optimization of renewables-based ammonia production, utilization, and distribution.



Prodromos Daoutidis is a College of Science and Engineering Distinguished Professor, holder of the Amundson Chair, and Executive Officer in the Department of Chemical Engineering and Materials Science at the University of Minnesota. He received a Diploma degree in Chemical Engineering from the Aristotle University of Thessaloniki, MSE degrees in Chemical Engineering and Electrical Engineering from the University of Michigan, and a Ph.D. in Chemical Engineering from the University of Michigan. He is the recipient of several awards, including the AIChE Computing in Chemical Engineering Award, the PSE Model Based Innovation Prize, and Best Paper Awards from the Journal of Process Control and Computers and Chemical Engineering. He is the Associate Editor for Process Systems Engineering in the AIChE Journal and an Associate Editor for the Journal of Process Control. He has co-authored five books and more than 300 refereed papers and has supervised to completion 33 Ph.D. students and five post-docs. His current research is on control and optimization of complex and networked systems, and the design and operation of distributed systems for renewable power generation and sustainable production of fuels and chemicals.



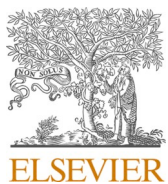
Qi Zhang is an Assistant Professor in the Department of Chemical Engineering and Materials Science at the University of Minnesota. He received his B.S. in Mechanical Engineering from RWTH Aachen University, his M.S. in Advanced Chemical Engineering from Imperial College London, and his Ph.D. in Chemical Engineering from Carnegie Mellon University. Prior to joining the University of Minnesota, he worked at BASF as a conceptual process engineer. His research interests lie in the development of efficient solution strategies for real-world optimization problems and data-driven discovery of unknown decision processes. Areas of application include sustainable energy and process systems, advanced manufacturing, supply chain engineering, and metabolic engineering. He is a recipient of the AIChE CAST W. David Smith Jr. Graduate Publication Award and NSF CAREER Award.

Update

Digital Chemical Engineering

Volume 10, Issue , March 2024, Page

DOI: <https://doi.org/10.1016/j.dche.2023.100121>



Contents lists available at ScienceDirect

Digital Chemical Engineering

journal homepage: www.elsevier.com/locate/dche



Corrigendum

Corrigendum to ‘Ammonia-based green corridors for sustainable maritime transportation’ [Digital Chemical Engineering 6 (2023) 100082]

Hanchu Wang, Prodromos Daoutidis^{*}, Qi Zhang^{*}

Department of Chemical Engineering and Materials Science, University of Minnesota, Minneapolis, MN 55455, USA



The authors regret that errors were present in the units for some of the numbers reported in their work. In the second paragraph of Section 4.1, ‘Gt’ should read ‘Mt’ and ‘GW’ should read ‘TWh’. The same applies

to the second paragraph of Section 5.

The authors would like to apologise for any inconvenience caused.

DOI of original article: <https://doi.org/10.1016/j.dche.2022.100082>.

* Corresponding authors.

E-mail addresses: daout001@umn.edu (P. Daoutidis), qizh@umn.edu (Q. Zhang).